XXVIII International Conference on Photonic, Electronic and Atomic Collisions (ICPEAC 2013) IOP Publishing
Journal of Physics: Conference Series **488** (2014) 012025 doi:10.1088/1742-6596/488/1/012025

X-ray lasing in diatomic molecules

Victor Kimberg, Song Bin Zhang and Nina Rohringer

Max Planck Institute for the Physics of Complex Systems, 01187 Dresden, Germany
Center for Free-Electron Laser Science, Luruper Chaussee 149, 22761 Hamburg, Germany

E-mail: `Victor.Kimberg@pks.mpg.de`

Abstract. We predict high-gain x-ray lasing in diatomic molecules by ultrafast core ionization of the C K- and O K-edges in CO and the N K-edge in N_2 with an x-ray free-electron laser source. To estimate the spectral and temporal output of this molecular x-ray laser, we solve generalized Maxwell-Bloch equations, keeping track of the electronic and nuclear degrees of freedom. Despite the broad fluorescence bandwidth, the amplified x-ray emission shows a narrow spectrum. By controlling the molecular alignment and thereby the alignment of the transition dipole moment polarization and emission energy control of the x-ray laser radiation is achievable.

1. Introduction

The quest to develop lasers at short wavelengths in the VUV and x-ray range based on atomic transitions to inner electronic shells is as old as the laser itself [1, 2, 3, 4]. The challenges for lasing on inner-shell transitions are the extremely short fs and sub-fs lifetimes of the electronic inner shell vacancies combined with relatively small transition dipole strengths. To achieve population inversion between the electronic valence and inner shells, pump rates have to be comparable to the decay rates of the vacancies, i.e. on the scale of fs^{-1}. The first proposed mechanism for creating a population inversion in the x-ray region is based on ultrafast inner-shell photoionization [1] and became possible [5] with the recent invention of x-ray free-electron laser (XFEL) sources [6]. Recently, an atomic inner-shell x-ray laser at 1.46 nm wavelength in atomic neon was demonstrated [7], using the LCLS XFEL source. In our previous studies [8, 9], we proposed an extension of this scheme to diatomic molecules, thereby extending the accessible photon-energy range from a quite limited number of atomic gas targets to a larger variety of molecular targets. We presented a feasibility study to obtain amplified x-ray emission (AXE) in N_2 [8] and the C and O core transitions in CO [9].

The study of x-ray lasing in molecules is the first step towards development of advanced spectroscopic methods like stimulated resonant inelastic x-ray scattering (SRIXS) [10, 11, 12]. For realization of SRIXS schemes, two x-ray colors are advantageous, separated by the typical excitation energies of the system of interest. Although schemes for seeded two-color XFEL sources in the hard x-ray regime have been proposed [13, 14, 15], the lack of a tunable two-color x-ray source with frequency separation beyond the SASE gain bandwidth seems to preclude SRIXS at present day XFELs. In that context, the molecular laser line combined with the tunable XFEL radiation results in a universal two-color x-ray radiation source. The amplified x-ray emission from the molecules containing C, N, and O atoms is particularly important for studying organic molecules due to their typical atomic constituents. The element and site

selective study of big molecules is possible in the x-ray range due to shifts of the atomic core-electron energies depending on the element and its chemical surrounding. Due to the additional nuclear degree of freedom, x-ray lasing in molecules offers new opportunities as compared to AXE in an atomic medium. The influence of vibrational dynamics on the x-ray amplification process is crucial [16, 8]. Here, we focused on lasing between molecular bound states and present calculations based on a generalized Maxwell-Bloch approach [8] in diatomic molecules. We treat both electronic and vibrational degrees of freedom, thereby revealing the importance of nuclear wave packet dynamics in stimulated x-ray processes. Our numerical results show that x-ray lasing in these molecules should be achievable at existing XFEL sources: For pulses of 50 fs duration, containing $\sim 10^{12}$ photons, high AXE gain is predicted in both cases, N_2 [8] and CO [9].

In the present paper we summarize our findings and focus on an advanced study of N_2 with a novel, detailed analysis of the dependence of the AXE on the angular distribution of a rotationally controlled molecular ensemble. We show that molecular alignment, achievable by using an additional optical laser pulse, considerably increases the gain. Moreover, control of the alignment of the dipole transition moment allows to target electronic transitions of different symmetries thereby controlling the polarization direction and photon energy of the emitted x-ray radiation. We analyse and compare the AXE process on several bound-bound transitions leading to different final ionic states with rather different potential energy curves, as well as value and orientation of the electronic transition dipole moments.

2. Theoretical model

The principles of AXE on the C K- and O K-edges of the CO and on the N K-edge of the N_2 are similar [8, 9]. Let us discuss AXE in diatomic molecules using N_2 as an example [8]. By tuning a focused XFEL beam above the K-edge of nitrogen (410 eV), a core hole in N_2 is produced by K-shell ionization. This core-excited intermediate state has a short lifetime of ≈ 6.6 fs [17], dominated by the Auger decay. If core-ionization rates are comparable to the Auger rate, a sizeable population inversion in molecular nitrogen can be achieved. Despite the small fluorescence yield in nitrogen, spontaneously emitted x-ray photons can get exponentially amplified, similarly to the atomic case [7]. The geometry of this single-pass x-ray amplifier is determined by the focus properties of the pump source. A long (5-10 mm), narrow (1.5 μm) focus of the XFEL, creates an elongated plasma channel of core inverted molecules. Fluorescence photons emitted at the entrance of the plasma channel stimulate radiative emission in direction of the propagating pump pulse and get exponentially amplified. Radiative decay of the core-ionized state proceeds mainly to three bound final states of the molecular ion (figure 1): $A^2\Sigma_g^+$, $B^2\Pi_u$, and $C^2\Sigma_u^+$. The transition to the C state is much weaker compared to the transition to the A and B states, as seen in synchrotron-based K-shell emission spectroscopy [18]. Due to this we focus on lasing transitions to the A (≈ 394.6 eV) and B (≈ 392.6 eV) states, which have different symmetries and as a result different orientation of the transition dipole moments.

Core ionization promotes the molecule to two nearly degenerate bound states $^2\Sigma_g^+$ and $^2\Sigma_u^+$ (figure 1) with core-holes on $1\sigma_g$ and $1\sigma_u$ orbitals, respectively. Owing to symmetry selection rules radiative decay of these states proceeds by two independent channels $^2\Sigma_u^+ \rightarrow A^2\Sigma_g^+$ and $^2\Sigma_g^+ \rightarrow B^2\Pi_u$ which are treated separately in our numerical calculations. It is important to note, that the $\Sigma \rightarrow \Sigma$ transition dipole moment (final state A) is oriented along the molecular axis, while the $\Sigma \rightarrow \Pi$ transition dipole moment (final state B) is oriented perpendicular to the molecular axis. In the case of a pre-aligned molecular ensemble the alignment of the transition dipole moment plays a crucial role: the $\Sigma \rightarrow \Sigma$ transitions are enhanced for molecules aligned perpendicular to the propagation direction of the XFEL and AXE fields, and suppressed for the anti-aligned ensemble. The situation is opposite in the case of $\Sigma \rightarrow \Pi$ transitions, for which lasing is enhanced for an ensemble of anti-aligned molecules and suppressed for an ensemble of

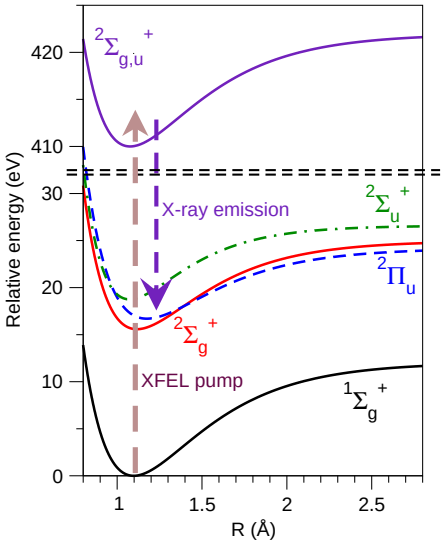

Figure 1. Potential energy curves of the ground state $^1\Sigma_g^+$, the intermediate core-ionized states $N1s^{-1}$ ($^2\Sigma_{g,u}^+$), and the final (valence ionized) states of N_2 [18]. The energy scale is relative to the energy of the ground state of the neutral molecule.

aligned molecules with respect to the AXE polarization. To model the AXE, we use a generalized Maxwell-Bloch approach [19], employing the paraxial wave approximation and assuming a slowly varying envelope of the electric field [20] for the propagation and amplification of the electric field associated with AXE. The polarization of the medium $\mathcal{P}_{if}$ is determined from the reduced density matrix of the cation governed by density matrix equations for an open quantum system. Detailed description of the theoretical approach can be found in [8, 9].

In the present paper we examine the effect of molecular alignment achieved with the help of an additional IR laser pulse. Dynamic alignment with intense laser pulses is a well established tool for preparing field-free aligned or oriented molecular ensembles [21, 22, 23]. We suppose that an optical, linearly polarized laser pulse dynamically aligns the ensemble of nitrogen molecules, thereby creating coherent rotational wave packets. By choosing the delay time between the optical and XFEL pulses, the molecular AXE process is studied for different molecular angular distributions. We suppose, that in first order, the AXE process is determined by the degree of the molecular alignment, which is defined by the expectation values of $\langle\cos^2\zeta\rangle$. Here ζ denotes the polar angle between the molecular axis and the electric-field vector of the linearly polarized laser field. We suppose that the molecular ensemble is well described by a thermal density matrix, before interaction with the optical alignment field. We employed the MCTDH code [24], to determine the time evolution of the rotational density matrix of the ensemble interacting with the optical pulse. Figure 2 (a) shows the expectation value of $\langle\cos^2\zeta\rangle$ as a function of time for the three initial temperatures, and (b) shows the molecular angular distribution function $\rho(\zeta)$ at the maxima and minima of the curves of figure 2 (a), corresponding to an ensemble of maximally aligned (the molecular axis is preferentially aligned with respect to the polarization axis of the optical pulse) and anti-aligned ensemble (the molecular axis is preferentially aligned in a plane perpendicular to the polarization axis of the optical pulse). In order to take into account the molecular alignment in the process of AXE, we average the nonlinear polarization $\mathcal{P}_{if}$ over the molecular distribution:

$$\langle\mathcal{P}_{if}(z,t)\rangle = 2\int_0^{\pi/2}\mathcal{P}_{if}(\theta;z,t)\rho(\zeta)\sin(\zeta)d\zeta. \quad (1)$$

Here the angle θ is the angle between the transition dipole moment and the polarization direction of the AXE field, and $\theta = \zeta$ in the case of $\Sigma \to \Sigma$ transitions, and $\theta = \pi/2 - \zeta$ in the case of $\Sigma \to \Pi$ transitions. The polarization vector of the IR alignment laser is supposed to be parallel to the AXE electric field polarization.

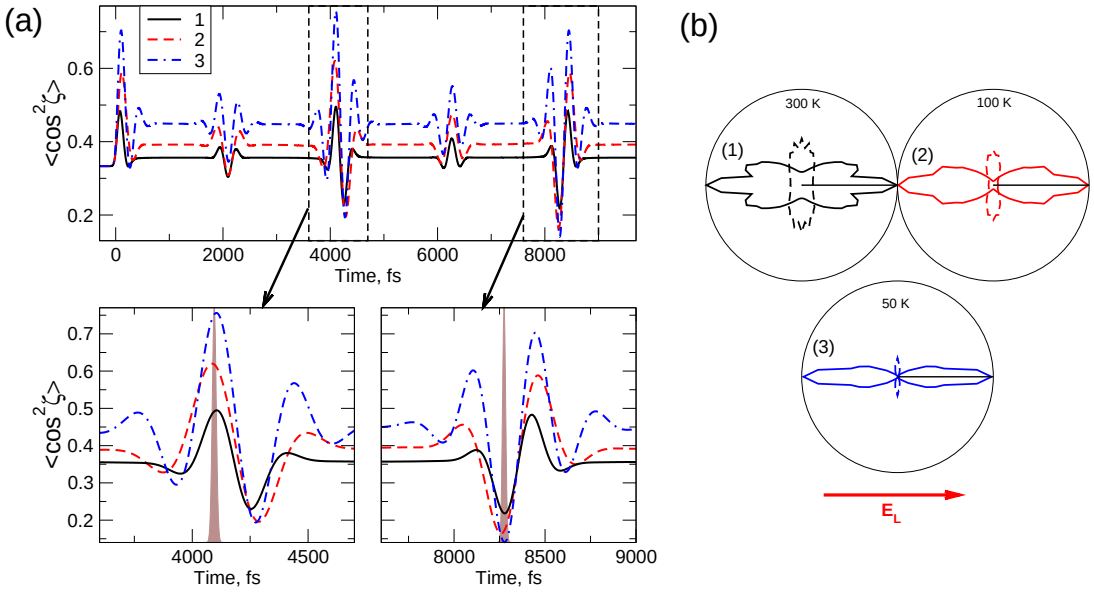

Figure 2. (a) Degree of molecular alignment $\langle\cos^2\zeta\rangle$ as a function of the time t_a relative to the peak intensity of the aligning optical pulse E_L computed using the rigid rotor model for the optical pulse of 800 nm wave length. Curves (1) and (2): pulse duration 110 fs and peak intensity 6×10^{13} W/cm^2, temperature 300 K (1) and 100 K (2); curve (3): 100 fs, 1×10^{14} W/cm^2, and 50 K, respectively. The shaded areas in the lower panels illustrate the temporal intensity profile of the pump XFEL pulse. (b) Angular distribution $\rho(\zeta)$ of the N_2 molecules relative to the polarization vector of the aligning field E_L at times related to the maxima (——) and minima (- - - -) of the corresponding $\langle\cos^2\zeta\rangle$ curves in panel (a): (1) $\langle\cos^2\zeta\rangle_{max}=0.5$ at $t_a=4110$ fs, $\langle\cos^2\zeta\rangle_{min}=0.22$ at $t_a=8280$ fs; (2) $\langle\cos^2\zeta\rangle_{max}=0.62$ at $t_a=4090$ fs, $\langle\cos^2\zeta\rangle_{min}=0.164$ at $t_a=8260$ fs; (3) $\langle\cos^2\zeta\rangle_{max}=0.77$ at $t_a=4108$ fs, $\langle\cos^2\zeta\rangle_{max}=0.14$ at $t_a=8280$ fs.

3. Results and discussions

Our theoretical simulations are performed assuming an XFEL pump pulse duration of $\tau=50$ fs containing 3.6×10^{12} photons, a focal radius of 1.5 μm, a gain medium of 5 mm length, and a molecular density of 2.5×10^{19} cm^{-3}. The dependence of the number of AXE photons on the propagation length for the $^2\Sigma_u^+\rightarrow A^2\Sigma_g^+$ and $^2\Sigma_g^+\rightarrow B^2\Pi_u$ lasing channels are shown in figure 3 (a). We compare the AXE efficiency of the two channels for an isotropic molecular ensemble, aligned and anti-aligned ensemble. It is clear, that molecular alignment is crucial and increases the AXE signal by several orders of magnitude (see table 1). According to the symmetry of the transition dipole moments, the x-ray lasing channel to the A state plays a major role in the case of the aligned molecular ensemble, for which $\Sigma\rightarrow\Sigma$ transition dipole moment is aligned parallel to the polarization of the optical laser and AXE fields. In contrast, in the case of an anti-aligned ensemble, characterized by a dipole moment oriented perpendicular to the optical laser polarization (pancake like angular distribution) the A channel is suppressed. In the case of an isotropic molecular ensemble the lasing channel to the B state is stronger than the lasing transition to the state A due to a generally larger number of contributing molecules lying in the plane orthogonal to the polarization vector. Let us also note that the AXE efficiency increases fast with increase of the degree of alignment in the case of the $^2\Sigma_u^+\rightarrow A^2\Sigma_g^+$ lasing transition (table 1) and reaches a value of 2.5×10^9 AXE photons ($\sim0.1\%$ conversion efficiency) at a degree of alignment $\langle\cos^2\zeta\rangle=0.77$. In the aligned ($\Sigma\rightarrow\Sigma$) or anti-aligned ($\Sigma\rightarrow\Pi$) case

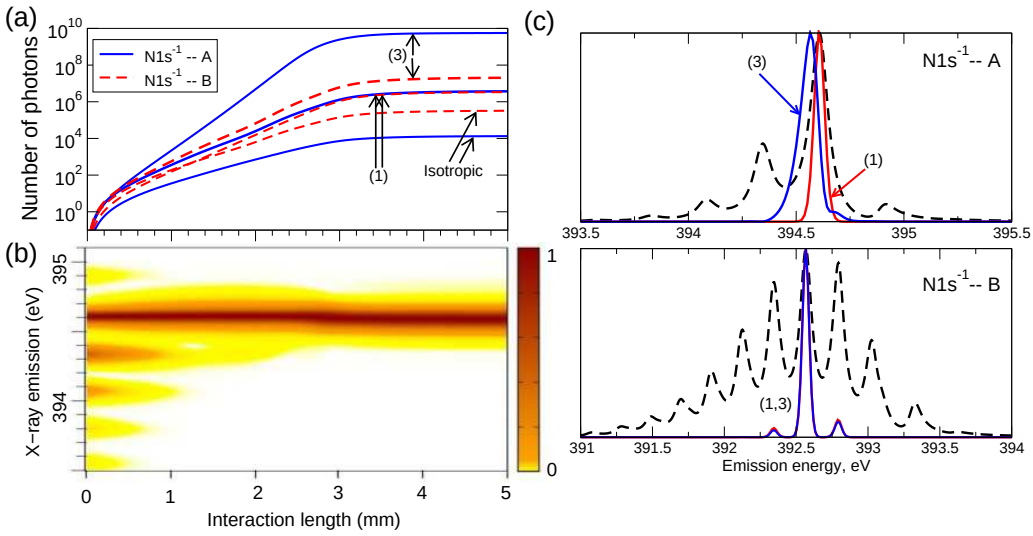

Figure 3. (a) Number of AXE photons vs interaction length for isotropic molecular distribution and pre-aligned molecular ensembles (see cases (1) and (3) in figure 2). (b) AXE spectrum at the $^2\Sigma_u^+ \rightarrow A^2\Sigma_g^+$ transition for an ensemble of aligned N_2 molecules with $\langle\cos^2\zeta\rangle = 0.77$ as a function of the propagation length. (c) X-ray fluorescence spectra (dashed lines) and AXE spectra at the end of the medium ($z = 5$ mm) (solid lines). The aligned ($^2\Sigma_u^+ \rightarrow A^2\Sigma_g^+$ channel) and anti-aligned ($^2\Sigma_g^+ \rightarrow B^2\Pi_u$ channel) ensembles are used here (see the cases (1) and (3) in figure 2).

the polarization of the emitted AXE field is along the polarization of the aligning IR laser. By varying the polarization of the aligning laser relative to the polarization of the XFEL the relative polarization of the XFEL and the AXE can be controlled.

Table 1. Number of AXE photons at the end of the medium $z = 5$ mm for isotropically distributed molecules and pre-aligned ensembles at the $^2\Sigma_u^+ \rightarrow A^2\Sigma_g^+$ and $^2\Sigma_g^+ \rightarrow B^2\Pi_u$ lasing channels. The alignment conditions (1), (2) and (3) are described in figure 2 caption.

Alignment:	Isotropic	300 K (1)		100 K (2)		50 K (3)	
$\langle\cos^2\zeta\rangle$	0.33	0.50	0.22	0.62	0.16	0.77	0.14
A $^2\Sigma_g^+$							
N_{phot}	1.3×10^4	3.6×10^6	548	2.7×10^8	122	2.5×10^9	58
B $^2\Pi_u$							
N_{phot}	3.2×10^5	1.3×10^4	3.7×10^6	1.4×10^3	1.3×10^7	176	2.0×10^7

The evolution of the AXE spectrum as a function of propagation length is illustrated in figure 3 (b) for the $^2\Sigma_u^+ \rightarrow A^2\Sigma_g^+$ channel using the degree of alignment $\langle\cos^2\zeta\rangle = 0.77$. Below the onset of the linear gain region ($z \ll 1$ mm), the AXE spectrum consists of several emission lines of transitions between vibrational sublevels, similar to the x-ray fluorescence spectrum (figure 3(c)). In the exponential gain region, a single transition energy ($\omega_L \approx 394.6$ eV)

picks up, suppressing the amplification of the other vibrational channels, so that at $z \approx 2$ mm, the spectrum transforms into a narrow line. The width of the line is determined by the natural lifetime broadening of the core-excited state. The AXE can be switched from channel ${}^2\Sigma_u^+ \rightarrow A^2\Sigma_g^+$ to ${}^2\Sigma_g^+ \rightarrow B^2\Pi_u$ by controlling the molecular alignment (see table 1). Such a control over the final electronic state in the AXE process allows to change the emission photon energy from 394.6 eV to 392.6 eV (see figure 3(c)). At saturation ($z > 2.5$ mm) the AXE line rebroadens (saturation broadening) and the line-shape is determined by nonlinear effects. Deep in saturation ($z \approx 4$ mm) the emission shifts towards lower energy and develops an asymmetric lineshape due to four-wave mixing of different vibrational transitions (figure 3 (c), curve (3)) [8].

4. Conclusions

Based on our theoretical estimates, x-ray lasing from N_2 pumped at the N K-edge and CO pumped at the C K- and O K-edges by high-intensity x-ray pulses seems realizable at presently available XFEL sources. We analyzed the dependence of the AXE intensity on the x-ray fluorescence spectrum, value and orientation of the electronic transition dipole moment and the duration of the pump pulse [8, 9]. Considerable increase of the amplified emission is achieved by pre-aligning of the molecular ensemble. Furthermore, the molecular gain medium offers a possibility of polarization control of the emitted x-ray radiation, by controlling the molecular alignment and thereby the alignment of the transition dipole moment. Unlike the broad x-ray fluorescence band, the AXE is emitted at a single vibrational transition. The AXE pulses have extremely narrow linewidth (~ 0.1 eV) and pulse duration shorter than the XFEL pump pulse (~ 30 fs). Tunability of the molecular laser line in conjunction with the tunable XFEL radiation results in a universal two-color x-ray radiation source, enabling advanced all x-ray pump-probe experiments. The present scheme can be applied to other homo- and heteronuclear diatomic systems, thereby extending the spectral range of this molecular-based x-ray lasing scheme.

References

[1] Duguay M A and Rentzepis G P 1967 *Appl. Phys. Lett.* **10** 350
[2] Matthews D L *et al* 1985 *Phys. Rev. Lett.* **54** 110
[3] Elton R C 1990 *X-ray lasers* (Academics)
[4] Suckewer S and Jaegle P 2009 *Laser Phys. Lett.* **6** 411
[5] Rohringer N and London R 2009 *Phys. Rev. A* **80** 013809
[6] Emma P *et al* 2010 *Nature Photon.* **4** 641
[7] Rohringer N *et al* 2012 *Nature* **481** 488
[8] Kimberg V and Rohringer N 2013 *Phys. Rev. Lett.* **110** 043901
[9] Kimberg V, Zhang S B and Rohringer N 2013 *J. Phys. B: At. Mol. Phys.* **46** 000000
[10] Hudis E, Shkolnikov P L and Kaplan A E 1994 *J. Opt. Soc. Am. B* bf 11 1158
[11] Sun Y-P, Liu J-C, Wang C-K and Gelmukhanov F 2010 *Phys. Rev. A* **81** 013812
[12] Weninger C *et al* 2013 *(to be published)*
[13] Geloni G, Kocharyan V and Saldin E 2011 *J. Mod. Opt.* **58** 1391
[14] Geloni G, Kocharyan V and Saldin E 2011 *Opt. Commun.* **284** 3348
[15] Lutman A A *et al* 2013 *Phys. Rev. Lett.* **110** 134801
[16] Miao Q, Liu J C, Ågren H, Rubensson J E and Gel'mukhanov F 2012 *Phys. Rev. Lett.* **109** 013809
[17] Kempgens B, Kivimäki A, Neeb M, Köppe H M, Brandshaw A M and Feldhaus J 1997 *J. Phys. B: At. Mol. Opt. Phys.* **29** 5389
[18] Glans P, Skytt P, Gunnelin K, Guo J H, and Nordgren J 1996 *Jour. of electr. spectr. and rel. phen.* **82** 193
[19] Kim C M, Janulewicz K A and Lee J 2011 *Phys. Rev. A* **84** 013834
[20] Fleck J A 1970 *Phys. Rev. B* **1** 84
[21] Stapelfeldt H and Seideman T 2003 *Rev. Mod. Phys.* **75** 543
[22] De S *et al* 2009 *Phys. Rev. Lett.* **103** 153002
[23] Xu N, Wu C, Huang J, Wu Z, Liang Q, Yang H and Gong Q 2006 *Opt. Exp.* **14** 4992
[24] Worth G A, Beck M H, Jäckle A and Meyer H-D *The MCTDH Package* Version 8.4 (2007), see http://mctdh.uni-hd.de